Oncology of CNS Tumors

Jörg-Christian Tonn
David A. Reardon
James T. Rutka
Manfred Westphal
Editors

Third Edition

Springer

Oncology of CNS Tumors

Jörg-Christian Tonn • David A. Reardon
James T. Rutka • Manfred Westphal
Editors

Oncology of CNS Tumors

Third edition 2019

Springer

Editors
Jörg-Christian Tonn
Department of Neurosurgery
University of Munich Department
of Neurosurgery
Munich
Germany

James T. Rutka
SickKids Hospital
University of Toronto
Toronto, ON
Canada

David A. Reardon
Dana-Farber Cancer Institute Center
Harvard University
Boston
USA

Manfred Westphal
Department of Neurosurgery
University of Hamburg
Hamburg
Germany

ISBN 978-3-030-04151-9 ISBN 978-3-030-04152-6 (eBook)
https://doi.org/10.1007/978-3-030-04152-6

Library of Congress Control Number: 2019935556

This Springer imprint is published by the registered company Springer Nature Switzerland AG
The registered company address is: Gewerbestrasse 11, 6330 Cham, Switzerland

Preface

Neurooncology has definitively evolved into a molecular-based medicine as many entities are now being diagnosed and classified using molecular signatures. Their clinical relevance has been validated by numerous large cohort studies. This led to a revision of the WHO Classification with major changes including the incorporation of new entities that are defined by histology and molecular features. Therefore, treatment concepts had to be revised and refined accordingly, reflecting the respective roles of microsurgery, chemo- and immunotherapies, and radiation oncology. Likewise, the progress of imaging techniques within the last years needed to be considered.

Thus, the third edition of this textbook had to be reorganized within the framework of the revised WHO Classification System and most chapters had to be thoroughly revised. We also added new chapters with focus on principal concepts of neurooncology and practical issues of patient care.

We gratefully acknowledge the contribution of all authors who are highly renowned international experts in their field as well as Meike Stoeck and Sushil Kumar Sharma with their team from Springer-Verlag for their excellent support and assistance.

Munich, Germany — Jörg-Christian Tonn
Boston, MA, USA — David A. Reardon
Toronto, ON, Canada — James T. Rutka
Hamburg, Germany — Manfred Westphal

Contents

Part I

General Aspects in Neurooncology

David A. Reardon, Manfred Westphal,
Jörg-Christian Tonn

1 Pathology and Classification of Tumors of the Central Nervous System

Guido Reifenberger, Ingmar Blümcke, Pieter Wesseling, Torsten Pietsch, and Werner Paulus

1.1 Introduction

1.1.1 Histologic Classification of Central Nervous System Tumors

Rudolf Virchow (1821–1902), the founder of cellular pathology, already separated the gliomas from the "psammomas," the "melanomas," and other "sarcomas" of the nervous system in 1864/1865 [160]. However, it was not before 1926 that Bailey and Cushing developed the first systematic classification scheme for gliomas and introduced the concept of brain tumor grading [5]. The first edition of the World Health Organization (WHO) classification of tumors of the nervous system was published in 1979 [171], followed by consecutive editions in 1993, 2000, and 2007. All these WHO classifications primarily relied on histologic criteria and basically followed the histogenetic principle proposed by Bailey and Cushing [5]. Based on morphologic and immunohistochemical features, each tumor entity was classified according to its presumed cell of origin. In addition to the histologic tumor typing, the WHO classification traditionally comprises a histologic grading according to a four-tiered scheme ranging from WHO grade I (benign) to WHO grade IV (malignant). The WHO grading is not equivalent to the histologic tumor grading commonly used in other fields of surgical pathology, but rather reflects an estimate of the presumed natural course of disease and the prognosis of the patient. In general, WHO grade I lesions include tumors with a minimal proliferative potential and the possibility of cure following surgical resection. Typical examples are pilocytic astrocytomas, subependymomas, myxopapillary

G. Reifenberger (✉)
Institute of Neuropathology, Heinrich Heine University, Düsseldorf, Germany
e-mail: reifenberger@med.uni-duesseldorf.de

I. Blümcke
Department of Neuropathology, University Hospital Erlangen, Erlangen, Germany
e-mail: Ingmar.Bluemcke@uk-erlangen.de

P. Wesseling
Department of Pathology, VU University Medical Center, Amsterdam, The Netherlands
Department of Pathology, Princess Máxima Center for Pediatric Oncology, Utrecht, The Netherlands
University Medical Center, Utrecht, The Netherlands
e-mail: p.wesseling@vumc.nl

T. Pietsch
Department of Neuropathology, University of Bonn Medical Center, Bonn, Germany
e-mail: t.pietsch@uni-bonn.de

W. Paulus
Institute of Neuropathology, University Hospital Münster, Münster, Germany
e-mail: paulusw@uni-muenster.de

J.-C. Tonn et al. (eds.), *Oncology of CNS Tumors*, https://doi.org/10.1007/978-3-030-04152-6_1

ependymomas of the cauda equina, a variety of neuronal and mixed neuronal-glial tumors, schwannomas, and most meningiomas. Tumors of WHO grade II are those with low mitotic activity but a tendency for recurrence. Diffuse astrocytomas, isocitrate dehydrogenase (IDH)-mutant, and oligodendrogliomas, IDH-mutant and 1p/19q-codeleted, are classic examples of WHO grade II tumors. WHO grade III is reserved for neoplasms with histologic evidence of anaplasia, generally in the form of increased mitotic activity, increased cellularity, nuclear pleomorphism, and cellular anaplasia. WHO grade IV is assigned to mitotically active and necrosis-prone highly malignant neoplasms that are typically associated with a rapid pre- and postoperative evolution of the disease. These include the glioblastomas and the various forms of embryonal tumors [88].

1.1.2 The WHO Classification 2016: Integrated Histologic and Molecular Classification

Histology-based classification allowed for meaningful separation of biologically and clinically distinct brain tumor entities and thus represented the diagnostic "gold standard" for many decades. However, the histogenetic concept of central nervous system (CNS) tumor classification has been challenged as for most tumors the actual cell of origin is still unknown. Experimental evidence from mouse models suggests that gliomas, for example, are more likely to arise from neural stem or progenitor cells rather than from terminally differentiated astrocytes or oligodendrocytes [141]. More importantly, it became evident that the rapidly growing knowledge on the diagnostic and/or prognostic value of particular genetic and epigenetic alterations in different tumor types needed to be included in an integrated morphologic and molecular approach for tumor classification [90]. Several studies reported that molecular classification of, e.g., adult gliomas correlates better with clinical outcome than histologic classification. In addition, it has become clear that certain tumor entities, including glioblastoma, correspond to a spectrum of genetically and biologically distinct tumor groups, whereas oligoastrocytomas lack distinctive genetic alterations but molecularly correspond to either astrocytic or oligodendroglial tumors.

The revised fourth edition of the WHO classification of CNS tumors of 2016 [89, 91] has considered these advances and employs a combination of histologic and molecular characteristics for the definition of several tumor entities, in particular among the gliomas and embryonal tumors (Table 1.1). This integrated "histomolecular" approach represents a paradigm shift and allows for a more reproducible diagnosis but also may cause new challenges, e.g., in terms of the required implementation of molecular diagnostic methods [97]. Moreover, it is important to be aware of the shortcomings of molecular tests. For example, for the diagnosis of "canonical" oligodendroglioma according to the WHO classification 2016, the tumor should have complete loss of both the short arm of chromosome 1 and of the long arm of chromosome 19 (whole arm 1p/19q codeletion), but, e.g., fluorescent *in situ* hybridization (FISH) analysis using one probe on 1p and one on 19q does not allow to discriminate partial from complete losses [164]. In certain situations, the molecular characteristics may actually override the histologic diagnosis in the integrated diagnostic approach. For instance, in a diffuse glioma with the histologic appearance of an astrocytoma, detection of the presence of *IDH1* or *IDH2* hotspot mutation combined with 1p/19q codeletion leads to the diagnosis of oligodendroglioma, IDH-mutant and 1p/19q-codeleted [91].

While tumor typing has been improved by diagnostic molecular markers in the WHO classification 2016, assessment of malignancy grades is still based on traditional morphologic criteria. Table 1.2 shows an overview of WHO grades assigned to major CNS tumor entities [91]. In most instances, WHO grading continues to provide important information on a tumor's malignancy

Table 1.1 WHO classification of tumors of the central nervous system 2016 (adapted from [91])

Diffuse astrocytic and oligodendroglial tumors	**Tumors of the cranial and paraspinal nerves**
Diffuse astrocytoma, IDH-mutant	Schwannoma
Gemistocytic astrocytoma, IDH-mutant	Cellular schwannoma
Diffuse astrocytoma, IDH-wild-type	Plexiform schwannoma
Diffuse astrocytoma, NOS	Melanotic schwannoma
Anaplastic astrocytoma, IDH-mutant	Neurofibroma
Anaplastic astrocytoma, IDH-wild-type	Atypical neurofibroma
Anaplastic astrocytoma, NOS	Plexiform neurofibroma
Glioblastoma, IDH-wild-type	Perineurioma
Giant cell glioblastoma	Hybrid nerve sheath tumors
Gliosarcoma	Malignant peripheral nerve sheath tumor (MPNST)
Epithelioid glioblastoma	Epithelioid MPNST
Glioblastoma, IDH-mutant	MPNST with perineurial differentiation
Glioblastoma, NOS	**Meningiomas**
Diffuse midline glioma, H3-K27M-mutant	Meningioma
Oligodendroglioma, IDH-mutant and 1p/19q-codeleted	Meningothelial meningioma
Oligodendroglioma, NOS	Fibrous meningioma
Anaplastic oligodendroglioma, IDH-mutant and 1p/19q-codeleted	Transitional meningioma
Anaplastic oligodendroglioma, NOS	Psammomatous meningioma
Oligoastrocytoma, NOS	Angiomatous meningioma
Anaplastic oligoastrocytoma, NOS	Microcystic meningioma
Other astrocytic tumors	Secretory meningioma
Pilocytic astrocytoma	Lymphoplasmacyte-rich meningioma
Pilomyxoid astrocytoma	Metaplastic meningioma
Subependymal giant cell astrocytoma	Chordoid meningioma
Pleomorphic xanthoastrocytoma	Clear cell meningioma
Anaplastic pleomorphic xanthoastrocytoma	Atypical meningioma
Ependymal tumors	Papillary meningioma
Subependymoma	Rhabdoid meningioma
Myxopapillary ependymoma	Anaplastic (malignant) meningioma
Ependymoma	**Mesenchymal, non-meningothelial tumors**
Papillary ependymoma	Solitary fibrous tumor/hemangiopericytoma
Clear cell ependymoma	Hemangioblastoma
Tanycytic ependymoma	Hemangioma
Ependymoma, *RELA* fusion-positive	Epithelioid hemangioendothelioma
Anaplastic ependymoma	Angiosarcoma
Other gliomas	Kaposi sarcoma
Chordoid glioma of third ventricle	Ewing sarcoma/peripheral primitive neuroectodermal tumor
Angiocentric glioma	Lipoma
Astroblastoma	Angiolipoma
Choroid plexus tumors	Liposarcoma
Choroid plexus papilloma	Desmoid-type fibromatosis
Atypical choroid plexus papilloma	Myofibroblastoma
Choroid plexus carcinoma	Inflammatory myofibroblastic tumor
Neuronal and mixed neuronal-glial tumors	Benign fibrous histiocytoma
Dysembryoplastic neuroepithelial tumor	Fibrosarcoma
Gangliocytoma	Undifferentiated pleomorphic sarcoma (UPS)/ malignant fibrous histiocytoma (MFH)
Ganglioglioma	Leiomyoma
Anaplastic ganglioglioma	Leiomyosarcoma

(continued)

Table 1.1 (continued)

Dysplastic gangliocytoma of cerebellum (Lhermitte-Duclos)	Rhabdomyoma
Desmoplastic infantile astrocytoma and ganglioglioma	Rhabdomyosarcoma
Papillary glioneuronal tumor	Chondroma
Rosette-forming glioneuronal tumor	Chondrosarcoma
Diffuse leptomeningeal glioneuronal tumor	Osteoma
Central neurocytoma	Osteochondroma
Extraventricular neurocytoma	Osteosarcoma
Cerebellar liponeurocytoma	**Melanocytic lesions**
Paraganglioma	Meningeal melanocytosis
Tumors of the pineal region	Meningeal melanocytoma
Pineocytoma	Meningeal melanoma
Pineal parenchymal tumor of intermediate differentiation	Meningeal melanomatosis
Pineoblastoma	***Lymphomas***
Papillary tumor of the pineal region	Diffuse large B-cell lymphoma (DLBCL) of the CNS
Embryonal tumors	Immunodeficiency-associated lymphoproliferative disorders of the CNS
Medulloblastoma, genetically defined	AIDS-related diffuse large B-cell lymphoma
Medulloblastoma, WNT-activated	EBV-positive diffuse large B-cell lymphoma, NOS
Medulloblastoma, SHH-activated and *TP53*-mutant	Lymphomatoid granulomatosis
Medulloblastoma, SHH-activated and *TP53*-wild-type	Intravascular large B-cell lymphoma
Medulloblastoma, non-WNT/non-SHH	
Medulloblastoma, group 3	Low-grade B-cell lymphomas of the CNS
Medulloblastoma, group 4	T-cell and NK/T-cell lymphomas of the CNS
Medulloblastoma, histologically defined	Anaplastic large cell lymphoma, *ALK*-positive
Medulloblastoma, classic	Anaplastic large cell lymphoma, *ALK*-negative
Medulloblastoma, desmoplastic/nodular	MALT lymphoma of the dura
Medulloblastoma with extensive nodularity	***Histiocytic tumors***
Medulloblastoma, large cell/anaplastic	Langerhans cell histiocytosis
Medulloblastoma, NOS	Erdheim-Chester disease
Embryonal tumor with multilayered rosettes, C19MC-altered	Rosai-Dorfman disease
Embryonal tumor with multilayered rosettes, NOS	Juvenile xanthogranuloma
Medulloepithelioma	Histiocytic sarcoma
CNS neuroblastoma	***Germ cell tumors***
CNS ganglioneuroblastoma	Germinoma
CNS embryonal tumor, NOS	Embryonal carcinoma
Atypical teratoid/rhabdoid tumor	Yolk sac tumor
CNS embryonal tumor with rhabdoid features	Choriocarcinoma
	Teratoma
	Mature teratoma
	Immature teratoma
	Teratoma with malignant transformation
	Mixed germ cell tumor
	Tumors of the sellar region
	Craniopharyngioma
	Adamantinomatous craniopharyngioma
	Papillary craniopharyngioma
	Granular cell tumor
	Pituicytoma
	Spindle cell oncocytoma
	Metastatic tumors

Provisional entities are printed in italics

Table 1.2 WHO grading of tumors of the CNS (adapted from [91])

Tumor group	Tumor entity	WHO grade I	WHO grade II	WHO grade III	WHO grade IV
Diffuse astrocytic and oligodendroglial tumors	Diffuse astrocytoma, IDH-mutant		o		
	Anaplastic astrocytoma, IDH-mutant			o	
	Glioblastoma, IDH-wild-type				o
	Glioblastoma, IDH-mutant				o
	Diffuse astrocytic glioma, IDH-wild-type,with molecular features of glioblastoma				o
	Diffuse midline glioma, H3-K27M-mutant				o
	Oligodendroglioma, IDH-mutant and 1p/19-codeleted		o		
	Anaplastic oligodendroglioma, IDH-mutant and 1p/19q-codeleted			o	
Other astrocytic gliomas	Pilocytic astrocytoma	o			
	Subependymal giant cell astrocytoma	o			
	Pleomorphic xanthoastrocytoma		o		
	Anaplastic pleomorphic xanthoastrocytoma			o	
Ependymal tumors	Myxopapillary ependymoma	o			
	Subependymoma	o			
	Ependymoma		o		
	Ependymoma, *RELA* fusion-positive		o	o	
	Anaplastic ependymoma			o	
Other gliomas	Angiocentric glioma	o			
	Chordoid glioma of the third ventricle		o		
Choroid plexus tumors	Choroid plexus papilloma	o			
	Atypical choroid plexus papilloma		o		
	Choroid plexus carcinoma			o	
Neuronal and mixed neuronal-glial tumors	Gangliocytoma	o			
	Ganglioglioma	o			
	Anaplastic ganglioglioma			o	
	Dysembryoplastic neuroepithelial tumor	o			
	Dysplastic gangliocytoma of the cerebellum	o			
	Desmoplastic infantile ganglioglioma	o			
	Central/extraventricular neurocytoma		o		
	Cerebellar liponeurocytoma		o		
	Papillary glioneuronal tumor	o			
	Rosette-forming glioneuronal tumor	o			
	Paraganglioma of the filum terminale	o			
Pineal parenchymal tumors	Pineocytoma	o			
	Pineal parenchymal tumor of intermediate differentiation		o	o	
	Pineoblastoma				o
	Papillary tumor of the pineal region		o	o	
Embryonal tumors	Medulloblastoma (all subtypes)				o
	ETMR, C19MC-altered				o
	Medulloepithelioma				o
	CNS neuroblastoma/ganglioneuroblastoma				o
	Atypical teratoid/rhabdoid tumor				o
Tumors of the cranial and peripheral nerves	Schwannoma	o			
	Neurofibroma	o			
	Perineurioma	o			
	MPNST		o	o	o

(continued)

Table 1.2 (continued)

Tumor group	Tumor entity	WHO grade I	WHO grade II	WHO grade III	WHO grade IV
Meningiomas	Meningioma	o			
	Atypical meningioma		o		
	Clear cell meningioma		o		
	Chordoid meningioma		o		
	Anaplastic meningioma			o	
	Papillary meningioma			o	
	Rhabdoid meningioma			o	
Mesenchymal, non-meningothelial tumors	Capillary hemangioblastoma	o			
	Solitary fibrous tumor/hemangiopericytoma	o[a]	o[a]	o[a]	
Tumors of the sellar region	Craniopharyngioma	o			
	Granular cell tumor	o			
	Pituicytoma	o			
	Spindle cell oncocytoma	o			

[a]Grading according to soft tissue tumor grade 1, 2, or 3

and the patient's prognosis. However, the relevance of histologic grading has been challenged in certain entities, including IDH-mutant diffuse astrocytomas and ependymal tumors [107, 161]. Thus, WHO grading likely needs to be refined by assessment of molecular markers in the future. For example, diffuse astrocytomas, IDH-wild-type, WHO grade II, that carry genetic alterations typical of glioblastoma, such as gain of chromosome 7 and loss of chromosome 10, *TERT* promoter mutation, or *EGFR* amplification, clinically behave like glioblastomas, IDH-wild-type, WHO grade IV [120, 163]. The term "diffuse astrocytic glioma, IDH-wild-type, with molecular features of glioblastoma, WHO grade IV" has been suggested for such cases, indicating that certain molecular markers may override histologic grading.

1.1.3 Immunohistochemistry in the Classification of Central Nervous System Tumors

Immunohistochemical staining for the expression of specific differentiation markers, mutant oncoproteins, as well as proliferation-associated antigens greatly facilitates CNS tumor classification. Table 1.3 provides a list of diagnostically helpful antigens that are commonly used for the differential diagnosis of different tumor entities or the assessment of proliferative activity. In the routine setting, immunohistochemistry is usually performed on formalin-fixed paraffin-embedded sections. Thereby, important differential diagnostic problems that are impossible to solve by conventional histology alone can be clarified. For example, the challenging differential diagnosis of malignant small, round, and blue cell tumors can often be solved by immunohistochemistry. In case of a metastasis of unknown primary, several markers are available that identify the organ site and type of the primary tumor. However, there are still a number of issues that cannot be solved by immunohistochemistry, such as the classification of oligoastrocytomas, which traditionally suffered from interobserver variability because specific immunohistochemical markers for neoplastic astrocytes or oligodendrocytes are missing [80, 156]. In addition, most markers (including GFAP) are expressed in both neoplastic and non-neoplastic cells, i.e., may not allow for the distinction between neoplastic and nonneoplastic/reactive cells.

To facilitate the histologic assessment of a tumor's malignancy grade, immunohistochemistry for the proliferation-associated antigen Ki-67 using the MIB1 antibody has become common practice. Although the MIB1 index does provide useful information in several circumstances, the fact that staining results and evaluation methods

are variable in different laboratories, together with the considerable overlap of MIB1 positivity in tumors of different WHO grades, has so far precluded the definition of defined cutoff values. Therefore, MIB1 staining isn't a criterion for grading in most tumor entities, except for meningioma, where a high MIB1 index is considered as evidence of atypia.

Importantly, immunohistochemistry using antibodies that detect tumor-specific aberrations, such as point mutations, loss of nuclear expression, or nuclear translocation of mutant proteins, may greatly facilitate diagnostics. Mutation-specific antibodies readily allow for the demonstration of relevant mutations like IDH1-R132H, H3-K27M, and BRAF-V600E. Other diagnostically relevant markers include loss of nuclear expression of ATRX, H3-K27me3, SMARCB1/INI1, or SMARCA4/BRG1, as well as aberrant nuclear staining for p53, STAT6, RELA, β-catenin, and others (Table 1.3). Thus, in many instances immunohistochemical markers allow for an integrated WHO diagnosis without the need of (cyto)genetic analyses [87, 111, 121, 149].

1.1.4 Molecular Markers for Central Nervous System Tumors

Diagnostic markers. WHO classification of CNS tumors requires immunohistochemical and/or molecular assessment of diagnostic markers, including IDH mutation, 1p/19q codeletion and H3-K27M mutation in diffuse gliomas, *C11orf95/RELA* fusion in supratentorial ependymomas, *C19MC* alteration in embryonal tumors

Table 1.3 Selected immunohistochemical markers used in CNS tumor classification

Markers for molecular characteristics of gliomas
Loss of nuclear ATRX staining, BRAF-V600E, H3-K27M nuclear staining, loss of nuclear H3-K27me3 staining, IDH1-R132H, L1CAM, p53 nuclear staining, RELA nuclear staining
Markers for molecular characteristics of embryonal tumors
β-Catenin nuclear staining, YAP1, GAB1, OTX2, $p75^{NGFR}$, LIN28A, BCOR, loss of nuclear SMARCB1/INI1 or SMARCA4/BRG1 staining
Glial and/or neuronal/neuroendocrine markers
GFAP, MAP2, OLIG2, S-100, synaptophysin, neurofilament proteins, NeuN, chromogranin A
Epithelial markers
Cytokeratins (pan-cytokeratins, various subtypes), desmoplakin, epithelial membrane antigen (EMA), TTF1 (carcinomas of the lung or thyroid, tumors of the neurohypophysis), napsin (bronchial adenocarcinoma), CDX2 (carcinomas of the (lower) gastrointestinal tract), prostate-specific antigen (PSA), thyreoglobulin, GATA3 (carcinomas breast or urothelial tract), estrogen and progesterone receptors, HER2/Neu (receptor status of breast cancer), CD10, PAX8 (renal cell carcinoma)
Melanocytic markers
Melan A, HMB-45
Mesenchymal markers
Vimentin, smooth muscle actin (SMA), desmin, myoglobin, myoD1, myogenin (skeletal muscle), STAT6 nuclear staining (solitary fibrous tumor/hemangiopericytoma), CD31, CD34 (endothelial)
Lymphocytic markers
CD45 (pan-leukocytes), CD19, CD20, CD79, PAX5 (B cells), CD3 (T cells), CD68, CD163, IBA-1, HLA-DR (monocytes, macrophages, microglia), CD138 (plasma cells), kappa/lambda light chains
Germ cell markers
β-HCG, alpha-fetoprotein (AFP), placental alkaline phosphatase (PLAP), human placental lactogen (HPL), OCT4, c-Kit, CD30
Pituitary hormones
Prolactin, ACTH, TSH, FSH, LH, GH
Proliferation marker
Ki-67 (MIB1)
Other useful markers
PD-L1 (predictive for immune checkpoint inhibition, e.g., in non-small cell lung cancer metastases)

Table 1.4 Selected molecular diagnostic tests used in CNS tumor classification

Genetic variables	Tumor type(s)
ATRX mutation*	IDH-mutant diffuse astrocytic gliomas (WHO grades II, III, and IV)
	H3-G34-mutant glioblastoma, IDH-wild-type anaplastic astrocytoma with piloid features
BRAF-V600E mutation*	PXA, ganglioglioma, DNT, pilocytic astrocytoma, glioblastoma, epithelioid, papillary craniopharyngioma
KIAA1549-BRAF fusion	Pilocytic astrocytoma, diffuse leptomeningeal glioneuronal tumor
C11orf95-RELA* fusion	**Ependymoma, RELA fusion-positive**
C19MC alteration*	**ETMR, C19MC-altered**
Chromosome 6 monosomy	Medulloblastoma, WNT-activated
Chromosome 7 gain & 10 loss	Glioblastoma, IDH-wild-type, *diffuse astrocytic glioma, IDH-wild-type, with molecular features of glioblastoma*
1p/19q codeletion	**Oligodendroglial tumors, IDH-mutant and 1p/19q-codeleted**
CTNNB1 mutation*	Medulloblastoma, WNT-activated, adamantinomatous craniopharyngioma
EGFR amplification	Glioblastoma, IDH-wild-type, *diffuse astrocytic glioma, IDH-wild-type, with molecular features of glioblastoma*
GNAQ or *GNA11* mutation	Meningeal (and uveal) melanocytic tumors
H3-K27M mutation*	**Diffuse midline glioma, H3-K27M-mutant**
H3-G34 mutation	*Glioblastoma, IDH-wild-type, H3-G34-mutant*
IDH mutation*	**Diffuse gliomas, IDH-mutant**
MGMT promoter methylation	Predictive marker for better response of glioblastoma, IDH-wild-type to DNA-alkylating chemotherapy
MYC/*MYCN* amplification	Poor prognosis in (subgroups of) medulloblastoma
NAB2-STAT6 fusion*	Solitary fibrous tumor/hemangiopericytoma
SMARCB1* or *SMARCA4* alteration	**Atypical teratoid/rhabdoid tumors**, peripheral nerve tumors associated with NF2 or schwannomatosis, epithelioid MPNST, poorly differentiated chordoma, CRINET
TERT promoter mutation	Oligodendroglial tumors, IDH-mutant and 1p/19-codeleted, glioblastoma, IDH-wild-type, clinically aggressive meningiomas
TP53* mutation	**Medulloblastoma, SHH-activated and *TP53*-mutant**, astrocytic gliomas, IDH-mutant or IDH-wild-type

List of genetic variables (left column) and associated tumor type(s). In some situations the genetic variables are part of the WHO 2016 definition of the tumor; these variables and tumors are listed in bold. Asterisks indicate markers that can (to some extent) be assessed by immunohistochemistry (see Table 1.3). Of note, the implications of finding a genetic variable in a CNS tumor should always be carefully interpreted in the clinical, radiological, and histopathological context. For instance, a tumor should only be called a diffuse midline glioma, H3-K27M-mutant when the tumor is a (1) diffusely infiltrative glioma, (2) located in the midline, and (3) carries the H3-K27M mutation. *ETMR* embryonal tumor with multilayered rosettes, *PXA* pleomorphic xanthoastrocytoma, *DNT* dysembryoplastic neuroepithelial tumor. Provisional or novel tumor types are printed in italics

with multilayered rosettes, and *SMARCB1/INI1* or *SMARCA4/BRG1* mutation and/or loss of nuclear expression in atypical teratoid/rhabdoid tumors (Table 1.4). The number of molecular markers providing diagnostic information is steadily increasing, e.g., mutation or loss of nuclear ATRX expression, *TERT* promoter mutation, *EGFR* amplification, gain of chromosome 7 and loss of chromosome 10, BRAF-V600E mutation, *KIAA1549-BRAF* fusions, and H3-G34 mutations (Table 1.4). In case that molecular analysis for required biomarkers is impossible or remains inconclusive, the term "NOS" (*not otherwise specified*) has been introduced in the WHO classification 2016 (Table 1.1). This term indicates that the diagnosis is based on histology only, i.e., that information on the relevant biomarker(s) is not available for an integrated diagnosis, e.g., due to limited availability of tissue [91]. NOS diagnoses should remain exceptional as they suffer from diagnostic uncertainty and individual treatment decisions may be more

difficult [97]. The term "not elsewhere classified (NEC)" has been proposed for tumors that cannot be assigned to any of the accepted WHO entities despite comprehensive molecular analyses were successfully performed [92]. Most commonly, NEC diagnosis is used in case of a mismatch between morphologic and molecular features or when new entities have been identified that are not yet included in the WHO classification 2016. In addition, NEC may be used when genetic findings not yet required for a specific WHO diagnosis are nonetheless considered important for classification [92].

Prognostic and predictive biomarkers. The *MGMT* promoter methylation status has gained clinical significance in neurooncology as a predictive marker for response to chemotherapy with DNA-alkylating drugs, in particular temozolomide, and longer survival of glioblastoma patients [165]. Hegi et al. [52] reported that patients with *MGMT* promoter-methylated glioblastoma responded significantly better to temozolomide treatment and survived longer than patients with *MGMT* promoter-unmethylated glioblastoma. *MGMT* testing is thus used to guide postoperative therapy, in particular in elderly glioblastoma patients, and to stratify patients into clinical trials evaluating novel therapies specifically for either *MGMT* promoter-methylated or promoter-unmethylated gliomas.

In addition to its role as diagnostic marker for oligodendroglioma, 1p/19q codeletion has been linked to benefit from the addition of procarbazine, lomustine, and vincristine (PCV) chemotherapy to upfront radiochemotherapy in anaplastic glioma patients and thus may guide treatment decisions in this patient population [162]. Similarly, detection of an IDH mutation is not only relevant for diagnostic purposes but identifies patients suitable for clinical trials evaluating treatments with mutant IDH inhibitors or peptide-based vaccination strategies [115, 136]. Molecular analyses may also be important to identify various other aberrant genes or signaling pathways that can be therapeutically targeted by small-molecule inhibitors or monoclonal antibodies, e.g., BRAF, MEK, NTRK1, ALK, or FGFR inhibitors, as well as antibodies targeting overexpressed EGFR or the EGFRvIII mutant protein [118].

High-throughput approaches. Due to the increasing demands for diagnostic assessment of more than single molecular markers, high-throughput techniques such as array-based comparative genomic hybridization, next-generation sequencing, as well as DNA methylation profiling have been implemented for parallel detection of multiple diagnostic, prognostic, or predictive markers, and such methods have been successfully evaluated for routine use in neurooncology. These methods allow for rapid, cost-effective, and comprehensive molecular analyses that provide valuable information beyond histology and represent an indispensable tool for individualized patient stratification in ongoing trials on novel molecularly targeted therapies [118]. A particularly powerful approach based on microarray-based DNA methylation profiling coupled with machine learning approaches has been recently reported that refines brain tumor classification to an unprecedented level of accuracy and reproducibility [24].

1.2 Diffuse Astrocytic and Oligodendroglial Tumors

The WHO classification 2016 groups together different entities under this header, including IDH-mutant astrocytic gliomas of WHO grades II, III, or IV, IDH-mutant and 1p/19q-codeleted oligodendroglial tumors of WHO grades II and III, IDH-wild-type glioblastomas, and H3-K27M-mutant diffuse midline gliomas (both WHO grade IV) (Table 1.1). In addition, IDH-wild-type diffuse and anaplastic astrocytomas are listed as provisional categories. Distinction of these different categories involves diagnostic assessments of defined molecular markers, in particular IDH mutation, 1p/19q codeletion, and H3-K27M mutation (Table 1.4). Testing for the most common IDH1-R132H mutation and the H3-K27M mutation can be accomplished by immunohistochemistry with mutation-specific antibodies. In addition, immunohistochemical

demonstration of loss of nuclear ATRX expression facilitates the distinction between IDH-mutant astrocytic and oligodendroglial tumors, while loss of nuclear positivity for trimethylated histone 3 lysin 27 (H3-K27me3) is typical for diffuse midline glioma, H3-K27M-mutant [87]. Detection of less common *IDH1* or *IDH2* mutations requires molecular genetic analyses, e.g., by DNA sequencing. Similarly, the 1p/19q codeletion status can only be determined by molecular (cyto)genetic analyses, such as fluorescent *in situ* hybridization (FISH), microsatellite analyses for loss of heterozygosity, multiplex ligation-dependent probe amplification (MLPA), or microarray-based techniques [98]. IDH-wild-type diffuse and anaplastic astrocytomas should be additionally tested for combined gain of chromosome 7 and loss of chromosome 10, *EGFR* amplification, and/or *TERT* promoter mutation to characterize tumors with molecular features of glioblastoma, IDH-wild-type [120]. Figure 1.1 shows an overview of the molecular diagnostic approach used for diffuse astrocytic and oligodendroglial tumors.

1.2.1 Diffuse Astrocytoma, IDH-Mutant

Definition. A slowly growing, diffusely infiltrating astrocytic glioma with a mutation affecting either IDH1 codon 132 or IDH2 codon 172 ("IDH mutation"). These tumors preferentially develop supratentorially in young adults and carry an intrinsic tendency for malignant progression to IDH-mutant anaplastic astrocytoma or IDH-mutant glioblastoma.

Incidence and age distribution. Diffuse astrocytomas, IDH-mutant, account for approximately 5% of CNS tumors and 10–15% of the astrocytic gliomas. They preferentially develop in young adults (age peak, 30–40 years).

Macroscopy and localization. Diffuse astrocytomas, IDH-mutant, predominantly grow in the cerebral hemispheres, in particular the frontal lobes. Macroscopically, they are ill-defined, gray to yellow, usually soft lesions in the white and/or gray matter. They enlarge preexisting structures and blur anatomical boundaries (Fig. 1.2a). Cystic changes are common.

Histopathology. Microscopy shows a well-differentiated astrocytic tumor of low to moderate cellularity and infiltrative growth. Mitotic activity is low. Necrosis and microvascular proliferation are absent. Most tumors are composed of multipolar neoplastic astrocytes with scant cytoplasm and fine cell processes that build a fibrillar glial matrix, often showing microcystic degeneration (Fig. 1.3a). *Gemistocytic astrocytoma*, *IDH-mutant*, is a variant characterized by tumor cells with enlarged eosinophilic cytoplasm, eccentric nuclei, and stout processes (Fig. 1.3b). To make the diagnosis, at least 20% of the tumor cells should demonstrate the gemistocytic phenotype. Diffuse astrocytomas (including gemistocytic astrocytoma), IDH-mutant, correspond to WHO grade II. As histologic signs of anaplasia may develop focally, selection of biopsy site and tissue sampling are important issues.

Immunohistochemistry. The tumors stain positive for glial fibrillary acidic protein (GFAP) and protein S-100. More than 90% carry the IDH1-R132H mutation [48] and express this mutant protein (Fig. 1.3d). Most tumors demonstrate widespread nuclear positivity for p53 (Fig. 1.3e) and loss of nuclear ATRX expression (Fig. 1.3f). The MIB1 index is low (<5%).

Differential diagnosis. Diffuse astrocytoma, IDH-mutant, is readily distinguished from reactive astrogliosis as well as IDH-wild-type astrocytic gliomas by the demonstration of an IDH mutation. Immunohistochemistry for ATRX and p53 can be helpful for distinction from oligodendroglial tumors. The differential diagnosis toward anaplastic astrocytoma, IDH-mutant, relies on histologic features of anaplasia, in particular elevated mitotic activity.

Molecular pathology. Missense mutations affecting codon 132 of IDH1 or, less commonly, codon 172 of IDH2 constitute the earliest aberration in these gliomas [23, 25, 147]. Any IDH mutation results in elevated levels of 2-hydroxyglutarate, which in turn leads to aberrant DNA and histone methylation, eventually causing a glioma CpG island methylator pheno-

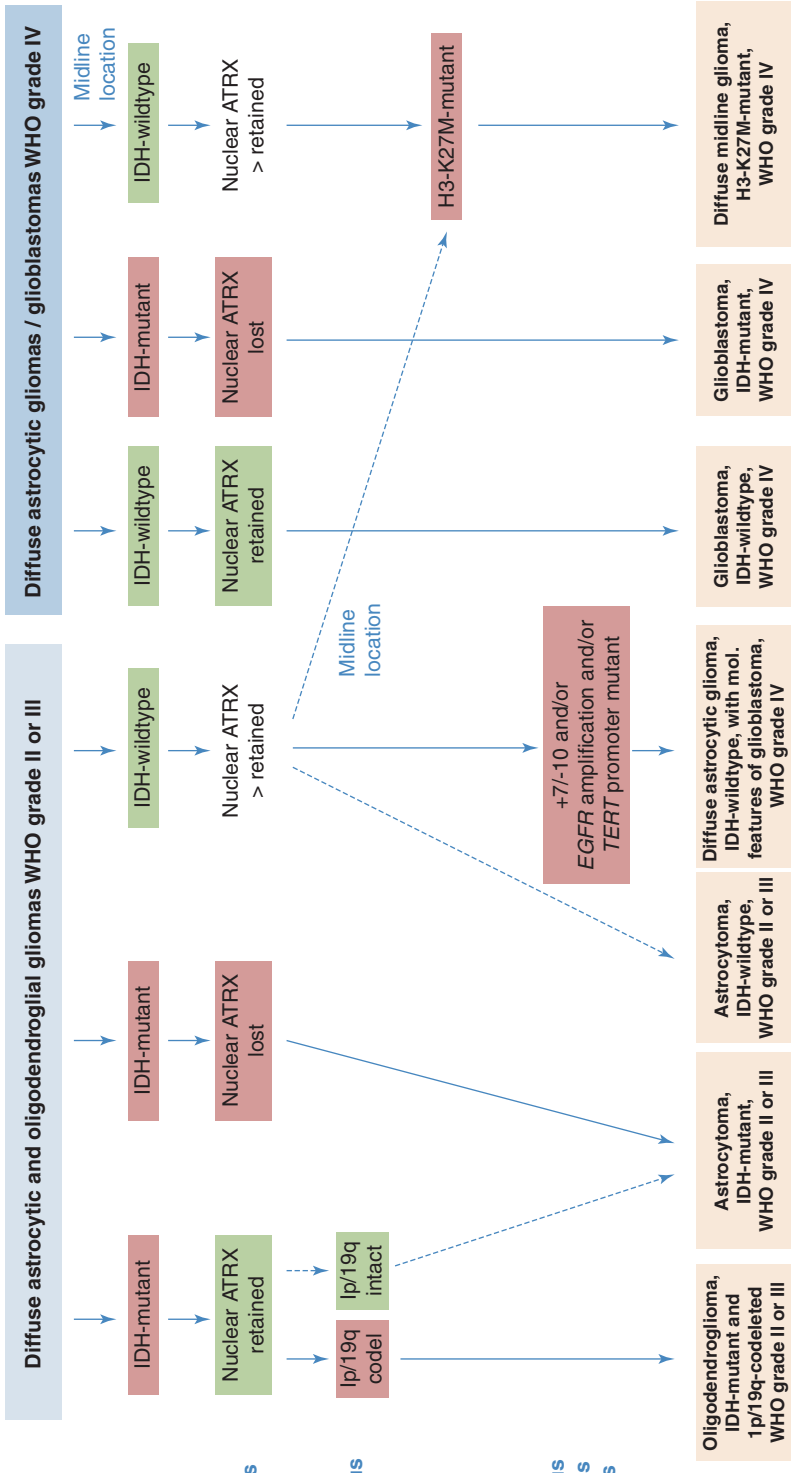

Fig. 1.1 Diagnostic approach commonly followed for WHO classification of diffuse astrocytic and oligodendroglial tumors (modified from [118])

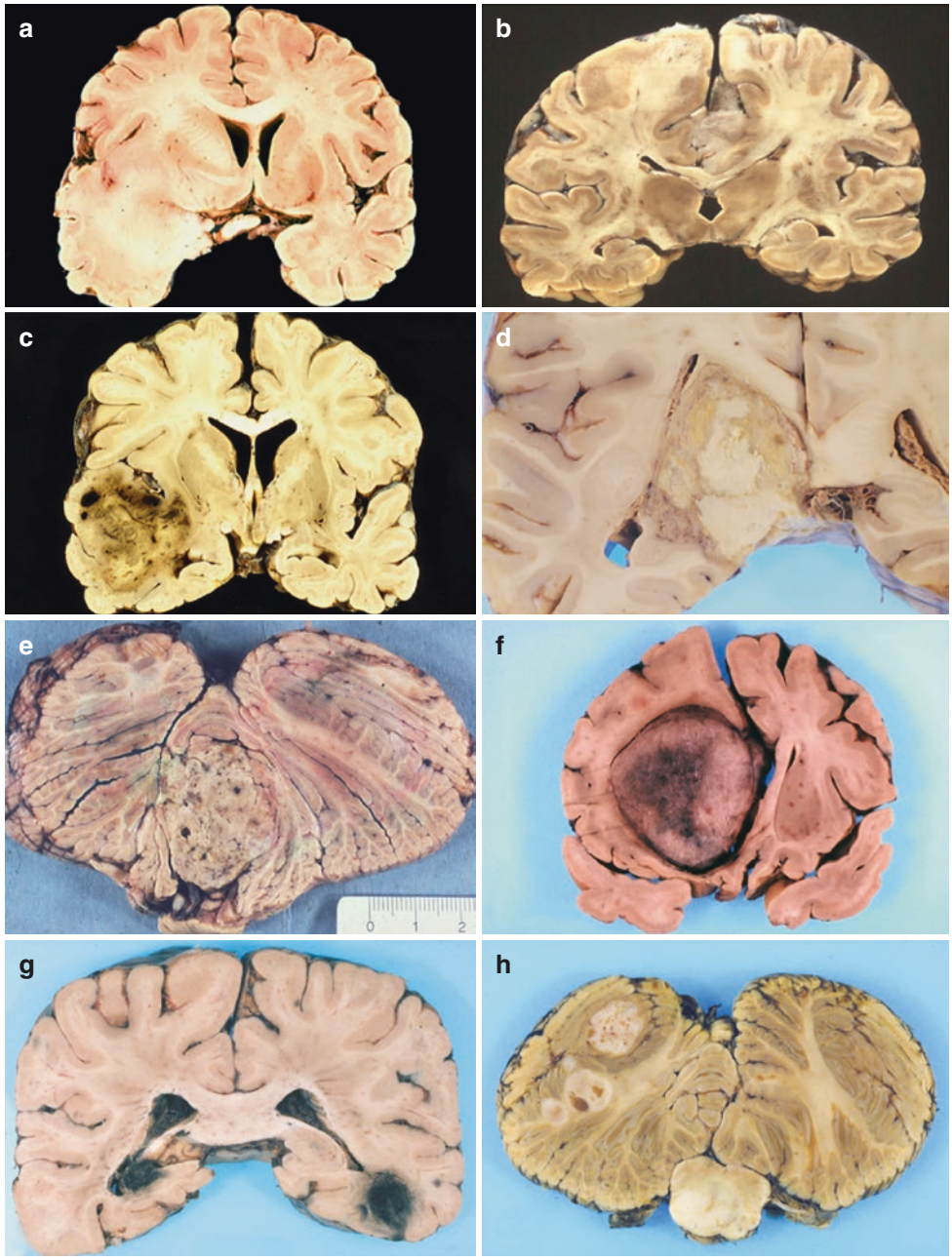

Fig. 1.2 Macroscopic appearance of selected types of primary and metastatic brain tumors. (**a**) Diffuse astrocytoma in the left temporal lobe. Note a diffuse mass lesion in the white matter without any distinct borders and blurring of the border between gray and white matter. (**b**) Oligodendroglioma involving the corpus callosum and cingulated gyrus on the right side. The tumor lacks any clear-cut borders and grows into the cortical gray matter. (**c**) Glioblastoma, IDH-wild-type, in the left temporal lobe with a heterogeneous cut surface demonstrating areas of necrosis and intratumoral hemorrhages. (**d**) Larger magnification of a glioblastoma showing large necroses in the tumor center. (**e**) Ependymoma in the fourth ventricle with complete obstruction of the ventricular lumen. Note that the tumor appears well demarcated from the surrounding cerebellar tissue. (**f**) Intraventricular meningioma in the left lateral ventricle. (**g**) Two distinct melanoma metastases in the brain. (**h**) Multiple metastases of a bronchial adenocarcinoma in the cerebellum and brain stem. (**i**) Dysplastic gangliocytoma of the cerebellum (Lhermitte-Duclos disease). Note enlargement of the cerebellar folia in the right hemisphere. (**j**) Diffuse leptomeningeal melanocytosis

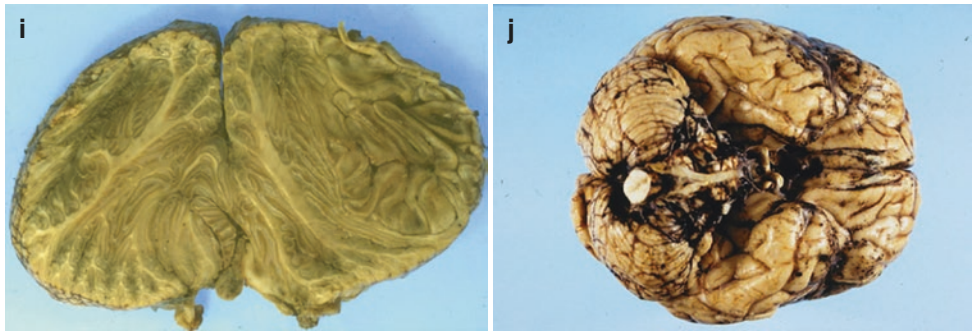

Fig. 1.2 (continued)

type (G-CIMP) [154]. IDH-mutant astrocytomas commonly carry *TP53* mutations associated with loss of heterozygosity on chromosome arm 17p, as well as *ATRX* mutations associated with loss of nuclear ATRX expression (Fig. 1.4a). *TERT* promoter mutations are restricted to a subset of tumors, while 1p/19q codeletion is absent by definition. Copy number gains of chromosome 7 or 7q are a common chromosomal imbalance in diffuse astrocytic gliomas, IDH-mutant, but gains and losses may also affect other chromosomes [163].

1.2.2 Anaplastic Astrocytoma, IDH-Mutant

Definition. An IDH-mutant astrocytic glioma with histologic features of anaplasia, in particular elevated mitotic activity. The tumors may arise from preexisting diffuse astrocytoma, IDH-mutant, but more commonly develop de novo, in the absence of a less malignant precursor lesion. They have an intrinsic tendency for progression to IDH-mutant glioblastoma.

Incidence and age distribution. Anaplastic astrocytomas, IDH-mutant, are similarly frequent as diffuse astrocytoma, IDH-mutant. The age distribution also overlaps, with a slightly later age peak between 35 and 45 years.

Macroscopy and localization. Anaplastic astrocytomas, IDH-mutant, are preferentially located in the cerebral hemispheres. Macroscopically, they are expanding lesions with perifocal edema. The distinction from normal brain tissue may be easier than in diffuse astrocytomas, but the borders are similarly ill-defined.

Histopathology. IDH-mutant anaplastic astrocytomas are characterized by signs of focal or diffuse anaplasia, such as increased cellularity, nuclear atypia, and in particular elevated mitotic activity (Fig. 1.3c). The histologic hallmarks of glioblastoma (microvascular proliferation and necrosis) are absent. Anaplastic astrocytomas, IDH-mutant, correspond to WHO grade III. However, the histologic distinction from diffuse astrocytoma, IDH-mutant, may be difficult in some cases, and grading criteria may need to be refined [161].

Immunohistochemistry. Anaplastic astrocytomas, IDH-mutant, share the immunohistochemical profile of diffuse astrocytoma, IDH-mutant. The MIB1 labeling index is increased (generally >5% positive tumor cells).

Molecular pathology. The mutational and copy number profile is similar to diffuse astrocytoma, IDH-mutant [23, 147, 163] (Fig. 1.4a). Genetic alterations associated with progression from diffuse (WHO grade II) to anaplastic (WHO grade III) astrocytoma are as yet poorly defined. A recent study indicated that *CDK4* amplification, *CDKN2A* deletion, and chromosome 14 loss are linked to less favorable outcome among patients with IDH-mutant astrocytic gliomas [27]. Other authors also reported on mutations, altered DNA methylation, and aberrant expression of cell-cycle regulatory genes as drivers of progression [25].

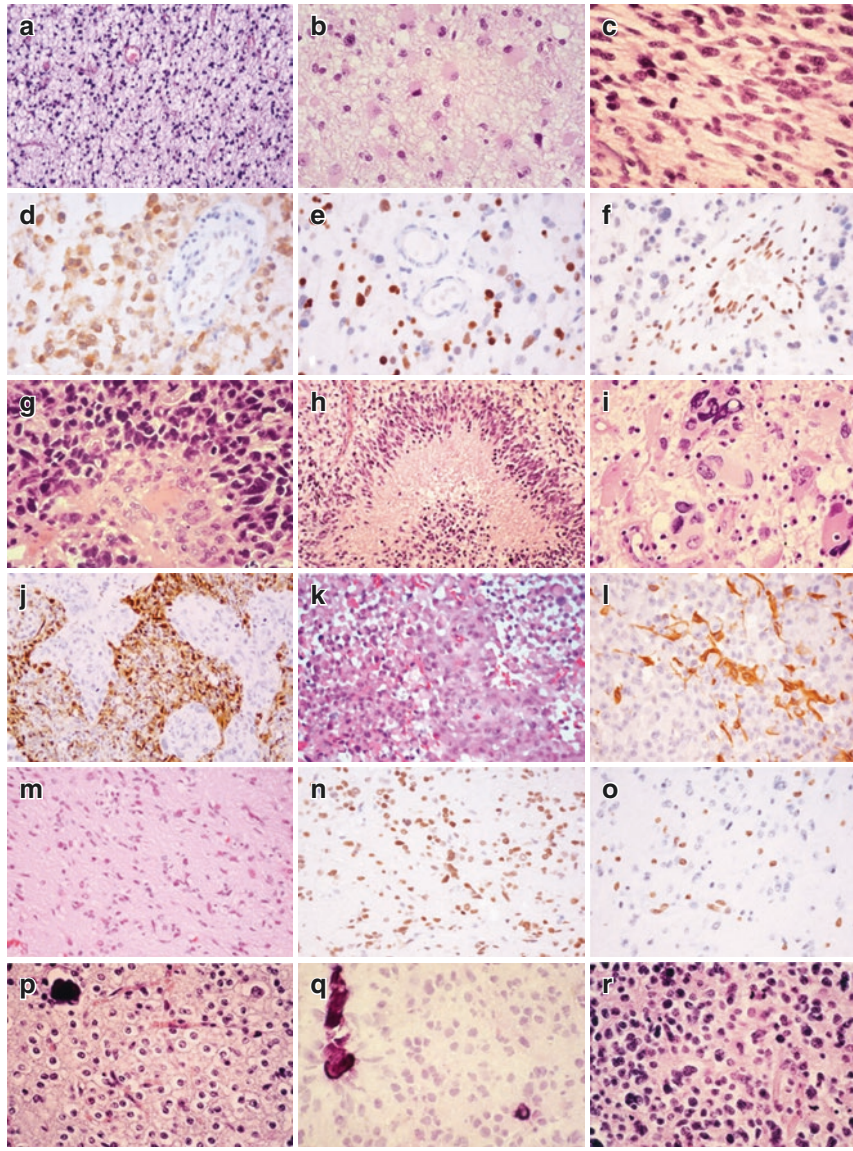

Fig. 1.3 Selected histologic and immunohistochemical findings in diffusely infiltrating astrocytic and oligodendroglial tumors. (**a**) Diffuse astrocytoma, IDH-mutant, WHO grade II (H&E). (**b**) Gemistocytic astrocytoma, IDH-mutant, WHO grade II (H&E). (**c**) Anaplastic astrocytoma, IDH-mutant, WHO grade III (H&E). Note increased cellularity, nuclear pleomorphisms, and mitotic activity. (**d–f**) Expression of IDH1-R132H (**d**) and nuclear p53 (**e**) as well as loss of nuclear ATRX immunopositivity in a diffuse astrocytoma, IDH-mutant. (**g**) Glioblastoma, IDH-wild-type, WHO grade IV. Highly cellular, pleomorphic glioma with mitotic activity and a pathological tumor vessel (H&E). (**h**) Typical necrosis with perinecrotic pseudopalisading in a glioblastoma, IDH-wild-type (H&E). (**i**) Giant cell glioblastoma, IDH-wild-type, WHO grade IV, with numerous multinucleated giant cells (H&E). (**j**) Gliosarcoma, IDH-wild-type, WHO grade IV. Note the biphasic pattern caused by GFAP-positive glial tumor areas and GFAP-negative sarcomatous tissue (GFAP). (**k**, **l**) Epithelioid glioblastoma, IDH-wild-type, WHO grade IV, composed of epithelioid tumor cells with eccentric nuclei (**k**, H&E) showing variable GFAP positivity (**l**). (**m–o**) Diffuse midline glioma, H3-k27M-mutant, WHO grade IV. Note a diffusely infiltrating astrocytic glioma (**m**, H&E) with nuclear staining for H3-K27M (**n**) and loss of nuclear H3-K27me3 positivity (**o**). (**p**, **q**) Oligodendroglioma, IDH-mutant and 1p/19q-codeleted, WHO grade II. (**p**) Oligodendroglioma-typical honeycomb appearance of tumor cells in formalin-fixed paraffin-embedded sections (H&E). (**q**) This artifact is not seen on frozen sections (H&E). (**r**) Anaplastic oligodendroglioma, IDH-mutant, WHO grade III. A cellular oligodendroglial tumor with anaplastic features including nuclear pleomorphism and mitotic activity

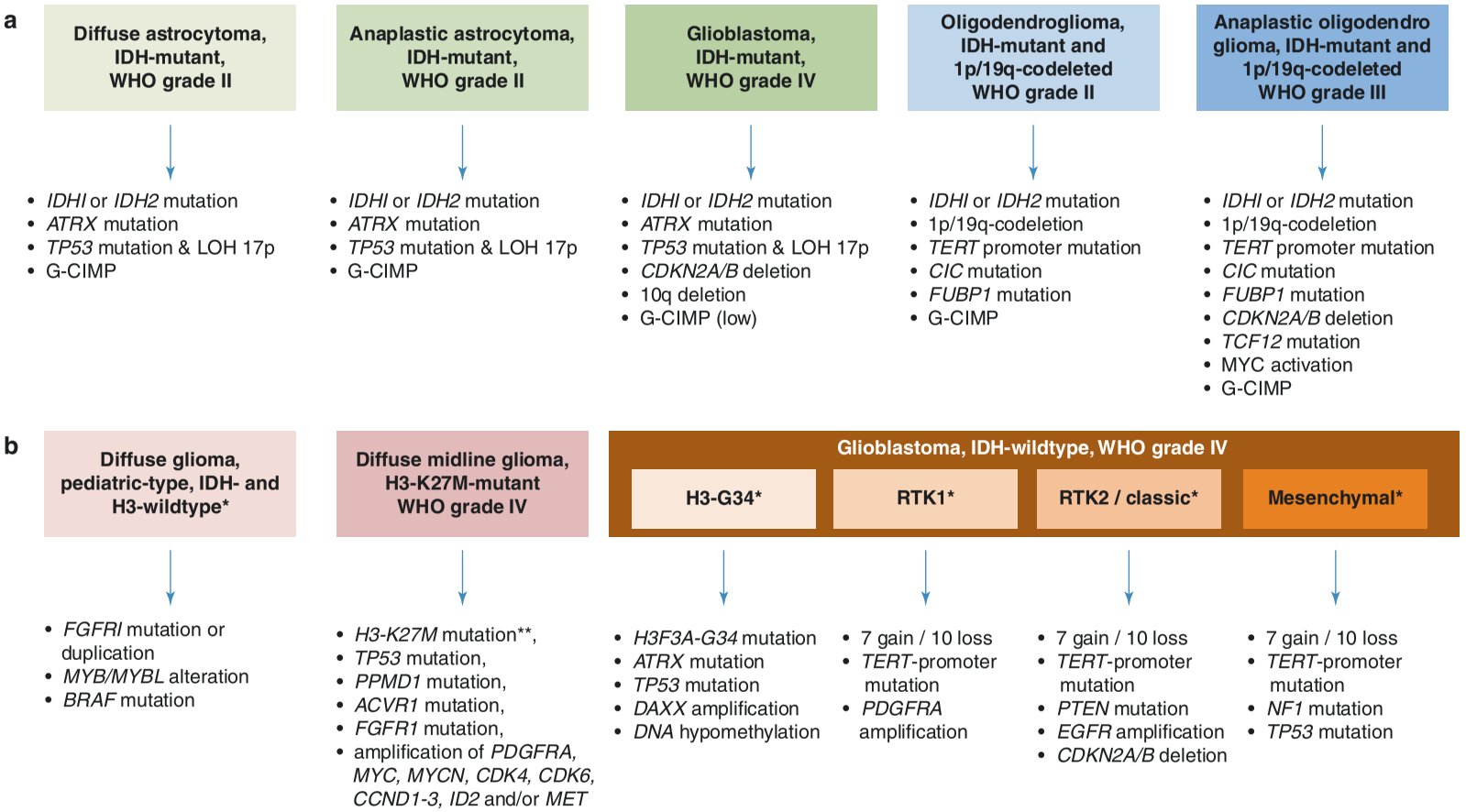

Fig. 1.4 Schematic representation of common genetic alterations detected in IDH-mutant (**a**) and IDH-wild-type (**b**) diffuse astrocytic and oligodendroglial tumors. *G-CIMP* glioma CpG island methylator phenotype, *LOH* loss of heterozygosity. Asterisk—Glioma entities and variants not yet recognized in the WHO classification 2016. Double asterisk—H3-K27M mutations most commonly affect the *H3F3A* gene but may less commonly alternatively affect the *HIST1H3B* or *HIST1H3C* genes

1.2.3 Glioblastoma, IDH-Mutant

Definition. An IDH-mutant astrocytic glioma with marked histologic features of anaplasia including elevated mitotic activity, microvascular proliferation, and/or spontaneous necrosis. Glioblastoma, IDH-mutant, may arise from a preexisting diffuse or anaplastic astrocytoma, IDH-mutant, but also presents *de novo*, i.e., without a history of a lower-grade precursor tumor.

Incidence and age distribution. Glioblastomas, IDH-mutant, account for less than 10% of all glioblastomas. With a mean age of 45 years at diagnosis, patients are typically younger compared to patients with IDH-wild-type glioblastoma.

Macroscopy and localization. Glioblastoma IDH-mutant preferentially develops in the cerebral hemispheres, most commonly in the frontal lobe. Macroscopically, the tumors are ill-defined lesions that diffusely infiltrate the surrounding brain tissue. Areas of necrosis may be visible but often are less pronounced as in IDH-wild-type glioblastomas.

Histopathology. IDH-mutant glioblastomas are diffusely infiltrating astrocytic gliomas with marked features of anaplasia, including high cellularity, increased nuclear atypia and cellular pleomorphism, mitotic activity, pathologic microvascular proliferation, and/or areas of necrosis, including palisading necroses. Thus, the histologic appearance corresponds to glioblastoma, IDH-wild-type. In cases that have relapsed from pretreated diffuse or anaplastic astrocytomas, distinction between treatment-induced necrosis (radiation necrosis) and spontaneous tumor necrosis may be difficult, and grading may need to rely on the presence of microvascular proliferation. Glioblastoma, IDH-mutant, corresponds to WHO grade IV, although patient survival is longer compared to glioblastoma, IDH-wild-type, and anaplastic astrocytoma, IDH-wild-type [47].

Immunohistochemistry. The immunohistochemical profile corresponds to that of diffuse and anaplastic astrocytomas, IDH-mutant. The MIB1 index is usually high.

Differential diagnosis. Distinction from IDH-wild-type glioblastoma is based on the demonstration of IDH mutation. Anaplastic oligodendroglioma differs by a 1p/19q codeletion in addition to IDH mutation. H3-K27M-mutant diffuse midline gliomas are IDH-wild-type but carry the H3-K27M mutation.

Molecular pathology. Molecular alterations are similar to IDH-mutant diffuse and anaplastic astrocytomas, including IDH mutation as well as frequent *TP53* and *ATRX* mutation (Fig. 1.4a). Alteration of cell-cycle regulatory genes, including *CDKN2A* deletion and *CDK4* amplification, has been associated with poor outcome [27]. Lower DNA methylation levels compared to IDH-mutant lower-grade gliomas have also been associated with more aggressive behavior [25].

1.2.4 Glioblastoma, IDH-Wild-Type

Definition. An IDH-wild-type diffusely infiltrating glioma with predominantly astrocytic differentiation, usually high cellularity, marked cellular pleomorphism, nuclear atypia, brisk mitotic activity, as well as microvascular proliferation and/or necrosis. Glioblastoma, IDH-wild-type, typically presents with a short clinical history and preferentially develops in the cerebral hemispheres.

Incidence and age distribution. Glioblastomas, IDH-wild-type, are the most common gliomas. They account for 10–15% of all intracranial tumors and 50–60% of the astrocytic gliomas. The annual incidence is approximately 3–4 new cases per 100,000 population. Glioblastomas, IDH-wild-type, may develop at any age, but adult patients are most commonly affected (peak incidence, 50–70 years).

Macroscopy and localization. These tumors typically develop in the cerebral hemispheres. Tumor spread into the basal ganglia or to the contralateral hemisphere is not uncommon. Glioblastomas, IDH-wild-type, located in the cerebellum or spinal cord are rare. Macroscopically, IDH-wild-type glioblastomas are largely necrotic masses with a peripheral zone of fleshy gray tumor tissue (Fig. 1.2c, d). Intratumoral hemorrhages are frequent. The surrounding brain tissue usually shows a marked edema.

Histopathology. Microscopy shows a cellular, highly anaplastic glioma that may be composed of cells with various morphologies, including fibrillar and gemistocytic cells, fusiform cells, epithelioid cells, small anaplastic cells, and multinuclear giant cells. Nuclear atypia is usually marked, and mitotic activity, including atypical forms, is prominent (Fig. 1.3g). The presence of microvascular proliferation and/or necrosis is essential for the diagnosis (Fig. 1.3g, h). Microvascular proliferation often results in glomerulum- or garland-like capillary structures. Vascular thrombosis is common. In addition to large ischemic necroses, which are macroscopically visible and appear as the non-enhancing central part of the tumor on neuroimaging, glioblastomas typically demonstrate smaller, often multiple, irregularly shaped band-like or serpiginous foci of palisading necrosis (Fig. 1.3h).

Variants of glioblastoma, IDH-wild-type. The WHO classification distinguishes two variants, namely, *giant cell glioblastoma* and *gliosarcoma*. In addition, *epithelioid glioblastoma* is considered as a provisional variant.

Giant cell glioblastoma is characterized by numerous pleomorphic, multinucleated giant cells that may be extremely bizarre and reach sizes up to 500 μm (Fig. 1.3i). Some giant cell glioblastomas demonstrate a collagen- and reticulin fiber-rich matrix. Lymphocytic infiltration is often prominent. Giant cell glioblastomas may show a more circumscribed growth compared to classic glioblastoma, IDH-wild-type.

Gliosarcomas are characterized by histologically distinct gliomatous and sarcomatous areas (Fig. 1.3j). The glial component corresponds to glioblastoma and is immunohistochemically positive for GFAP. The sarcomatous tumor parts are rich in reticulin fibers and composed of GFAP-negative spindle cells, often resembling fibrosarcoma. Occasional cases may show evidence of chondroid, osseous, or myogenic differentiation. Epithelial metaplasia has also been reported.

Epithelioid glioblastomas are composed of epithelioid and sometimes rhabdoid tumor cells that are variably GFAP-positive (Fig. 1.3k, l). Their histologic features overlap with those of anaplastic pleomorphic xanthoastrocytoma. Recent data questioned that these tumors are a biologically distinct group but show that they molecularly stratify into three established entities [77].

Grading. Glioblastoma, IDH-wild-type, and its variants correspond to WHO grade IV.

Immunohistochemistry. Glioblastomas are usually positive for GFAP and protein S-100. Nuclear p53 immunoreactivity can be detected in 30–40% of the cases, with giant cell glioblastomas being more commonly p53-positive. Strong expression of the epidermal growth factor receptor (EGFR) is found in about 60% of the tumors. Immunostaining for IDH1-R132H is negative, and nuclear ATRX expression is typically retained; however, it may be lost in rare instances, e.g., the H3-G34-mutant glioblastomas. In patients older than 55 years, absence of IDH1-R132H staining is sufficient for the diagnosis of an IDH-wild-type glioblastoma [91]. In younger patients and patients with a lower-grade precursor tumor, sequencing of *IDH1* and *IDH2* is required to exclude other, less common IDH mutations. The MIB1 index is usually high but may show marked regional heterogeneity.

Differential diagnosis. The presence of microvascular proliferation and/or necrosis distinguishes glioblastoma, IDH-wild-type, from anaplastic astrocytoma, IDH-wild-type, although molecular alterations in the latter commonly correspond to those in glioblastomas (see below). The differential diagnosis toward IDH-mutant astrocytic tumors depends on the IDH status. Giant cell glioblastoma and epithelioid glioblastoma needs to be distinguished from anaplastic pleomorphic xanthoastrocytoma.

Molecular pathology. IDH-wild-type glioblastomas in adults are characterized by frequent gain of chromosome 7, loss of chromosome 10, *TERT* promoter mutations, mutation of the phosphatase and tensin homolog on chromosome 10 (*PTEN*) gene, homozygous deletion of the *CDKN2A/p14*^{ARF} and *CDKN2B* genes, and many other, less common alterations such as mutations in the *TP53*, *PIK3CA*, PI3K regulatory subunit 1 *(PIK3R1)*, and neurofibromatosis type 1 (*NF1*) genes [118]. Amplification of *EGFR* is detectable in 40–50% of the tumors, while amplification

of *PDGFRA*, *MET*, *CDK4*, *CDK6*, *MDM2*, and *MDM4* is seen in smaller subsets of tumors. About 50% of the *EGFR*-amplified glioblastomas carry on oncogenic deletion rearrangement (EGFRvIII) that encodes a constitutively active receptor lacking the external domain parts encoded by exons 2–7. BRAF-V600E mutation is overall rare in glioblastoma, IDH-wild-type, but found in about 50% of epithelioid glioblastomas [71].

Studies based on large-scale molecular profiling have indicated that glioblastoma, IDH-wild-type, comprises biologically distinct subgroups that can be separated by specific DNA methylation profiles associated with defined signature mutations and gene expression profiles [18, 24, 145]. Figure 1.4b shows a schematic representation of major molecular subgroups of glioblastoma and the most commonly associated genetic alterations.

1.2.5 Diffuse and Anaplastic Astrocytoma, IDH-Wild-Type

IDH-wild-type diffuse astrocytoma, WHO grade II, and anaplastic astrocytoma, WHO grade III, are considered as provisional entities in the WHO classification 2016 [89, 91]. In adults, most of these tumors carry genetic alterations typical for IDH-wild-type glioblastoma, such as gain of chromosome 7 and loss of chromosome 10, *TERT* promoter mutation, *EGFR* amplification, and others [23, 120, 148, 163]. Clinical behavior of these tumors closely corresponds to glioblastoma, IDH-wild-type, indicating that they represent histologically underdiagnosed glioblastomas, and thus may be better classified as *diffuse astrocytic glioma*, *IDH-wild-type*, *with molecular features of glioblastoma*. Alternatively, DNA methylation and copy number profiling can readily identify such tumors as distinct types of IDH-wild-type glioblastoma [24]. A smaller subset of IDH-wild-type diffuse astrocytomas, in particular those arising in children, correspond genetically to other entities, including *diffuse gliomas with BRAF*, *FGFR1*, or *MYB/MYBL* alterations that usually show an indolent clinical behavior following resection (Fig. 1.4b). In addition, rare tumors may correspond to newly delineated entities like *anaplastic astrocytoma with piloid features* [119].

1.2.6 Diffuse Midline Glioma, H3-K27M-Mutant

Definition. A diffusely infiltrating glioma with predominantly astrocytic differentiation located in CNS midline structures, in particular the thalamus, pons, brain stem and spinal cord, and carrying a K27M missense mutation in a histone 3 protein encoded either by *H3F3A*, *HIST1H3B*, or *HIST1H3C*.

Incidence and age distribution. Data on incidence of this newly defined entity are not available. Most tumors present in children and adolescents. However, adults may also be affected, in particular by thalamic and spinal tumors.

Macroscopy and localization. By definition, these tumors are located in CNS midline structures including the thalamus, pons, brain stem, and spinal cord. Occasional tumors may involve the cerebellum. The tumors are macroscopically ill-defined and cause enlargement of the involved anatomical structures. Areas of necrosis may be present.

Histopathology. The tumors present as diffusely infiltrative gliomas of predominantly astrocytic differentiation (Fig. 1.3m). Some tumors present histologically as low-grade lesions with monomorphic tumor cells, moderate cellularity, and low mitotic activity, while others show features of frank malignancy, including high cellularity and pleomorphism, mitotic activity, microvascular proliferation, and necrosis. Independent of histologic differentiation, diffuse midline glioma, H3-K27M-mutant, corresponds to WHO grade IV.

Immunohistochemistry. The tumor cells demonstrate nuclear immunoreactivity with antibodies against H3-K27M and loss of nuclear immunoreactivity for the trimethylated lysine at codon 27 of histone 3 (H3-K27me3) (Fig. 1.3n, o). Immunoreactivity for OLIG2, S-100, and MAP2 is common, while GFAP positivity may

be variable. Loss of nuclear ATRX expression is restricted to a minor subset, while nuclear p53 staining is common. MIB1 labeling is variable depending on cellularity and degree of differentiation.

Differential diagnosis. Other types of diffuse gliomas are distinguished by the absence of the disease-defining H3-K27M mutation. Rare instances of H3-K27M mutations in other types of gliomas, e.g., ependymomas or gliomas located outside of midline structures, do not suffice for the diagnosis of diffuse midline glioma, H3-K27M-mutant [87].

Molecular pathology. The diagnostic hallmark is a K27M mutation in *H3F3A*, *HIST1H3B*, or *HIST1H3C*, with mutations in the latter two genes being mostly restricted to pontine tumors. The H3-K27M mutation leads to aberrant recruitment of the polycomb repressive complex 2 and inhibition of the histone methyltransferase EZH2, which in turn causes loss of H3K27 trimethylation [7, 85]. In addition, mutations in *TP53* or *PPMD1* are frequently present as are amplifications of *PDGFRA*, *MYC*, *MYCN*, *CDK4*, *CDK6*, or cyclin D (*CCND1-3*) genes, *ID2*, or *MET* (Fig. 1.4b). Activin receptor 1 gene (*ACVR1*) mutations are seen in a subset of pontine tumors, while *FGFR1* alterations are found mostly in thalamic tumors [118].

1.2.7 Oligodendroglioma, IDH-Mutant and 1p/19q-Codeleted

Definition. A diffusely infiltrating, slowly growing glioma with IDH mutation and 1p/19q codeletion.

Incidence and age distribution. The annual incidence of oligodendroglial tumors, IDH-mutant and 1p/19q-codeleted (including anaplastic forms), is approximately 0.3 per 100,000 individuals. About 5–10% of all gliomas are oligodendroglial tumors. The incidence peaks between 35 and 45 years of age. These tumors are rare in children.

Macroscopy and localization. Most tumors arise in the cerebral hemispheres, most commonly the frontal lobe. The tumor mass is typically located in the white matter, but extension into the cerebral cortex is common. Rarely, oligodendrogliomas develop in the cerebellum, brain stem, or spinal cord. Macroscopically, the tumors appear as soft masses of grayish-pink color (Fig. 1.2b). Calcifications are frequently found. Areas of mucoid degeneration, cystic changes, and intratumoral hemorrhages are not unusual.

Histopathology. IDH-mutant and 1p/19q-codeleted oligodendrogliomas are moderately cellular, diffusely infiltrating gliomas of WHO grade II that are composed of isomorphic cells with round, hyperchromatic nuclei. After formalin fixation and embedding in paraffin, oligodendroglial tumor cells suffer from artifactual swelling that results in clear cells with central spherical nuclei and well-defined cell borders, the so-called honeycomb appearance (Fig. 1.3p). This diagnostically useful artifact is absent in smear preparations and frozen sections (Fig. 1.3q), thus making a definite intraoperative diagnosis difficult. Oligodendrogliomas may contain small gemistocytic cells that are GFAP-positive. A bona fide astrocytic tumor component may be present and is compatible with the diagnosis when molecular analysis shows IDH mutation and whole arm 1p/19q codeletion. Microcalcifications in the tumor tissue and/or the surrounding brain are common. Other degenerative features include extracellular mucin deposition and microcyst formation. Oligodendroglioma, IDH-mutant and 1p/19q-codeleted, shows a typical vascularization pattern that consists of a dense network of branching capillaries resembling the pattern of chicken wire. Infiltration of the cortex is frequent, with tumor cells forming secondary structures, such as perineuronal satellitosis, perivascular aggregations, and subpial accumulations.

Immunohistochemistry. Oligodendrogliomas are positive for S-100, MAP2, and Olig2. GFAP-positive small gemistocytes and gliofibrillary oligodendrocytes may be present. IDH1-R132H positivity is seen in the majority of tumors, and nuclear ATRX expression is generally retained, while nuclear p53 staining is absent or sparse. The MIB1 index is low (<5%).

Differential diagnosis. Differential diagnosis against macrophage-rich reactive lesions (demyelinating diseases or cerebral infarcts) as well as other tumor types that may present with clear cells, such as clear cell ependymoma, neurocytoma, dysembryoplastic neuroepithelial tumor (DNT), clear cell meningioma, and metastatic clear cell carcinoma, is accomplished by demonstration of IDH mutation and 1p/19q codeletion.

Molecular pathology. The combination of IDH mutation and 1p/19q codeletion defines these tumors. The characteristic whole arm 1p and 19q codeletion is due to an unbalanced t(1;19)(q10;p10) translocation [46, 61]. Losses of chromosome 4 are the second most common chromosomal aberration [27]. Most tumors additionally carry *TERT* promoter mutations (Fig. 1.4a), while *ATRX* and *TP53* mutations are typically absent [23, 25, 147]. Mutations in the *Drosophila homolog of capicua* (*CIC*) gene on 19q are also common, while mutations in the far upstream element-binding protein 1 gene (*FUBP1*) on 1p are restricted to about one third of tumors. IDH-mutant and 1p/19q-codeleted oligodendrogliomas demonstrate G-CIMP and *MGMT* promoter methylation [118].

1.2.8 Anaplastic Oligodendroglioma, IDH-Mutant and 1p/19q-Codeleted

Definition. An oligodendroglioma, IDH-mutant and 1p/19q-codeleted, with focal or diffuse histologic features of anaplasia.

Incidence and age distribution. Anaplastic oligodendrogliomas account for about half of the IDH-mutant and 1p/19q-codeleted oligodendroglial tumors. The age distribution overlaps with oligodendroglioma, IDH-mutant and 1p/19q-codeleted, and peaks in the fifth decade.

Macroscopy and localization. Tumors are usually located in the cerebral hemispheres with a preference for the frontal lobe, followed by the temporal lobe. Macroscopic appearance is similar to WHO grade II oligodendrogliomas. In some cases, areas of necrosis may be seen.

Histopathology. Anaplastic oligodendrogliomas are diffusely infiltrating cellular gliomas with histologic signs of anaplasia, including obvious mitotic activity (Fig. 1.3r), microvascular proliferation, and necrosis with or without pseudopalisading. The typical honeycomb cells and the vascular pattern of oligodendrogliomas are still recognizable. Microcalcifications may be seen. Gliofibrillary oligodendrocytes and minigemistocytes are common. Some cases may show marked cellular pleomorphism. An astrocytic component in an IDH-mutant and 1p/19q-codeleted tumor does not argue against the diagnosis of an oligodendroglial tumor. Anaplastic oligodendroglioma, IDH-mutant and 1p/19q-codeleted, corresponds to WHO grade III and is associated with shorter survival as compared to oligodendroglioma, IDH-mutant and 1p/19q-codeleted [27]. It has been suggested that presence of microvascular proliferation and necrosis is associated with shorter survival within the group of anaplastic oligodendroglioma, IDH-mutant and 1p/19q-codeleted [33].

Immunohistochemistry. The immunohistochemical profile is similar to WHO grade II oligodendrogliomas. GFAP-positive cells are more common and proliferative activity is increased.

Differential diagnosis. The differential diagnosis versus other types of high-grade gliomas, including malignant small cell astrocytic neoplasms, is readily solved by the demonstration of IDH mutation and 1p/19q codeletion.

Molecular pathology. The molecular profile is similar to oligodendroglioma, IDH-mutant and 1p/19q-codeleted (Fig. 1.4a). Alterations that have been linked to aggressive clinical behavior are 9p21 (*CDKN2A/B*) deletion, *TCF12* mutation, and activation of MYC signaling [3, 69, 83].

1.2.9 Oligoastrocytoma and Anaplastic Oligoastrocytoma, NOS

The WHO classification 2016 no longer considers oligoastrocytic gliomas as distinct entities as they lack specific genetic profiles but either carry genotypes of diffuse astrocytic or oligodendrog-

lial gliomas [131]. Only when molecular testing remains inconclusive or not possible and histology shows both astrocytic and oligodendroglial phenotypes, tumors may be classified as oligoastrocytoma, NOS, or anaplastic oligoastrocytoma, NOS. Individual tumors with histologic features of an oligoastrocytoma and genetically distinct cell populations showing molecular features of diffuse astrocytoma, IDH-mutant, or oligodendroglioma, IDH-mutant and 1p/19q-codeleted, have been reported, but these *oligoastrocytomas with dual genotype* are not recognized as distinct WHO entity [89, 91].

1.3 Other Astrocytic Tumors

1.3.1 Pilocytic Astrocytoma

Definition. A slowly growing, well-circumscribed, and frequently cystic astrocytoma of children and young adults. Histologic characteristics include a biphasic growth pattern of loose and compact tissue, Rosenthal fibers, and eosinophilic granular bodies. Biologically, pilocytic astrocytoma constitutes a single pathway disease characterized by genetic alterations in MAPK pathway genes.

Incidence and age distribution. Pilocytic astrocytomas account for 5–6% of all gliomas. Children and young adults are preferentially affected. Pilocytic astrocytomas are the most common primary brain tumors in pediatric patients. Patients with neurofibromatosis type 1 have an increased risk for pilocytic astrocytomas, in particular optic nerve gliomas. However, most pilocytic astrocytomas are sporadic tumors.

Macroscopy and localization. More than 80% are cerebellar tumors. Other typical sites include the optic nerve and optic chiasm, hypothalamus, thalamus, basal ganglia, brain stem, and spinal cord. Rare cases originate in the cerebral hemispheres. Macroscopically, pilocytic astrocytomas are soft, gray, frequently cystic lesions that are well-circumscribed. Local involvement of the leptomeninges may be seen.

Histopathology. Pilocytic astrocytomas are characterized by low to moderate cellularity and a biphasic architecture, consisting of compact areas with bipolar (piloid) tumor cells and microcystic areas with multipolar tumor cells (Fig. 1.5a). Rosenthal fibers and eosinophilic granular bodies are common (Fig. 1.5b). Capillary proliferation, degenerative cellular pleomorphism, foci of non-palisading necrosis, and occasional mitoses are still consistent with this diagnosis. However, high mitotic activity and palisading necrosis indicate that the tumor behaves more aggressively. Such rare cases may correspond to *anaplastic astrocytoma with piloid features* [119].

Pilomyxoid astrocytoma is a variant characterized by a monomorphic population of bipolar neoplastic astrocytes in a myxoid matrix. The tumor cells form pseudorosette-like angiocentric architectures (Fig. 1.5c). Rosenthal fibers are often missing. Pilomyxoid astrocytomas are predominantly found in the optic chiasms/hypothalamus region of children and associated with a higher risk of local recurrence and CSF seeding [152]. Intermediate forms between pilocytic and pilomyxoid astrocytoma have been reported [66].

Immunohistochemistry. Pilocytic astrocytomas are positive for GFAP, OLIG2, MAP2, and protein S-100. Immunostaining for p53 remains negative or restricted to individual cells. MIB1 labeling is usually low (<5%).

Differential diagnosis. The most important differential diagnosis is piloid gliosis, which may be found as a reaction to slowly growing tumors, such as craniopharyngioma or capillary hemangioblastoma, vascular malformations, as well as other chronic CNS lesions. In the spinal cord, tanycytic ependymoma is a rare differential diagnosis. Gangliogliomas are a common clinical differential diagnosis in long-standing, well-circumscribed lesions of the temporal lobe. However, the histologic demonstration of neoplastic ganglion cells clearly separates ganglioglioma from pilocytic astrocytomas.

Molecular pathology. Pilocytic astrocytomas are characterized by genetic alterations leading to aberrant activation of the MAPK pathway (Fig. 1.6a). Most common are in-frame fusions of the *KIAA1549* gene with the *BRAF* gene that activate BRAF signaling [28]. Less frequent are fusion genes involving other MAPK pathway genes like *RAF1*, *PTPN11*, or *NTRK2* and mutations in

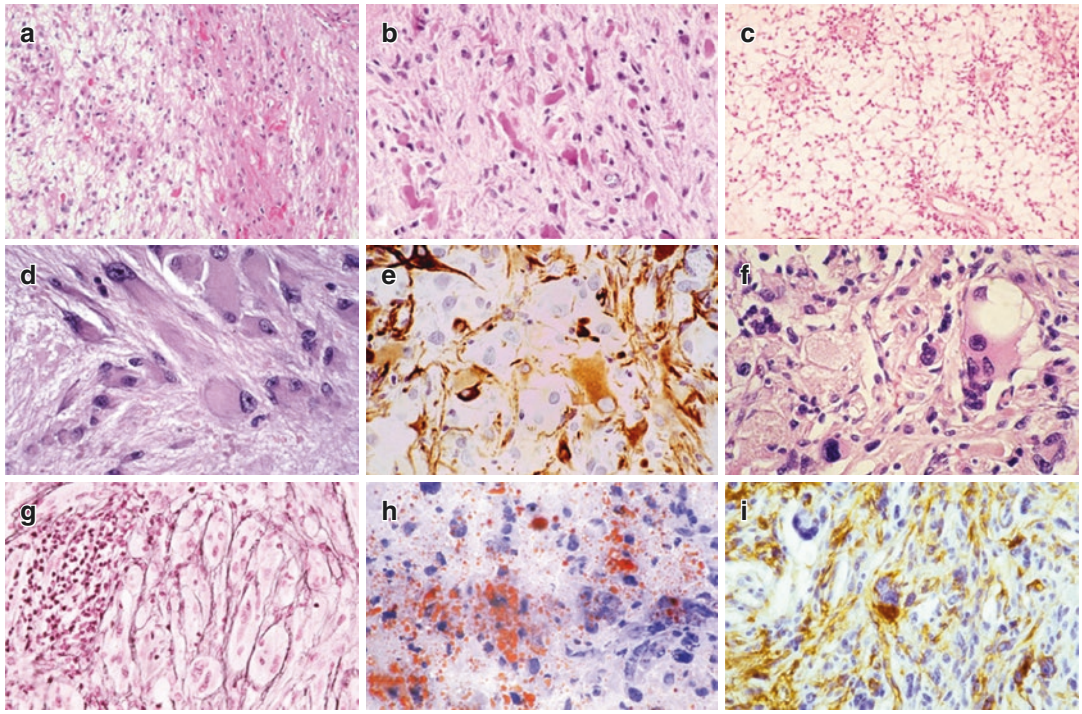

Fig. 1.5 Selected histologic and immunohistochemical features of other astrocytic gliomas. (**a**) Pilocytic astrocytoma, WHO grade I, showing a typical biphasic architecture with compact areas of bipolar (piloid) tumor cells and microcystic areas of multipolar tumor cells (H&E). (**b**) Numerous Rosenthal fibers in a pilocytic astrocytoma (H&E). (**c**) Pilomyxoid astrocytoma with perivascular tumor cell arrangements and myxoid degeneration of the tumor matrix (H&E). (**d**) Subependymal giant cell astrocytoma, WHO grade I. Histology shows a moderately cellular tumor composed of astrocytic cells with abundant eosinophilic cytoplasm and enlarged ganglion cell-like nuclei (H&E). (**e**) Variable expression of GFAP in a subependymal giant cell astrocytoma. (**f–i**) Pleomorphic xanthoastrocytoma, WHO grade II. (**f**) Histology shows pleomorphic tumor cells with cytoplasmic vacuolization (H&E). (**g**) Pericellular reticulin network and lymphocytic infiltrates (Gomori stain). (**h**) Lipidization of tumor cells (oil red stain). (**i**) Strong expression of CD34

BRAF, *KRAS*, *FGFR1*, or *NF1* [65]. The combination of MAPK gene alterations with *CDKN2A* deletion and *ATRX* mutation is typical for *anaplastic astrocytoma with piloid features* [119].

1.3.2 Subependymal Giant Cell Astrocytoma

Definition. A slowly growing tumor composed of large ganglionic astrocytes, typically arising in the wall of the lateral ventricles. Subependymal giant cell astrocytoma (SEGA) is closely associated with the tuberous sclerosis complex.

Incidence and age distribution. SEGAs typically manifest in the first two decades of life. Approximately 5–15% of patients with tuberous sclerosis develop SEGAs.

Macroscopy and localization. SEGAs are located in the wall of the lateral ventricles, often adjacent to the foramen of Monro. Hydrocephalus caused by blockade of this foramen is a common feature. Macroscopically, SEGAs are discrete intraventricular masses that frequently contain calcifications. The tumors are well vascularized and may show spontaneous intratumoral hemorrhage.

Histopathology. SEGAs are circumscribed, moderately cellular tumors composed of pleomorphic large astrocytic or ganglioid cells with abundant glassy eosinophilic cytoplasm and round, vesicular nuclei with distinct nucleoli

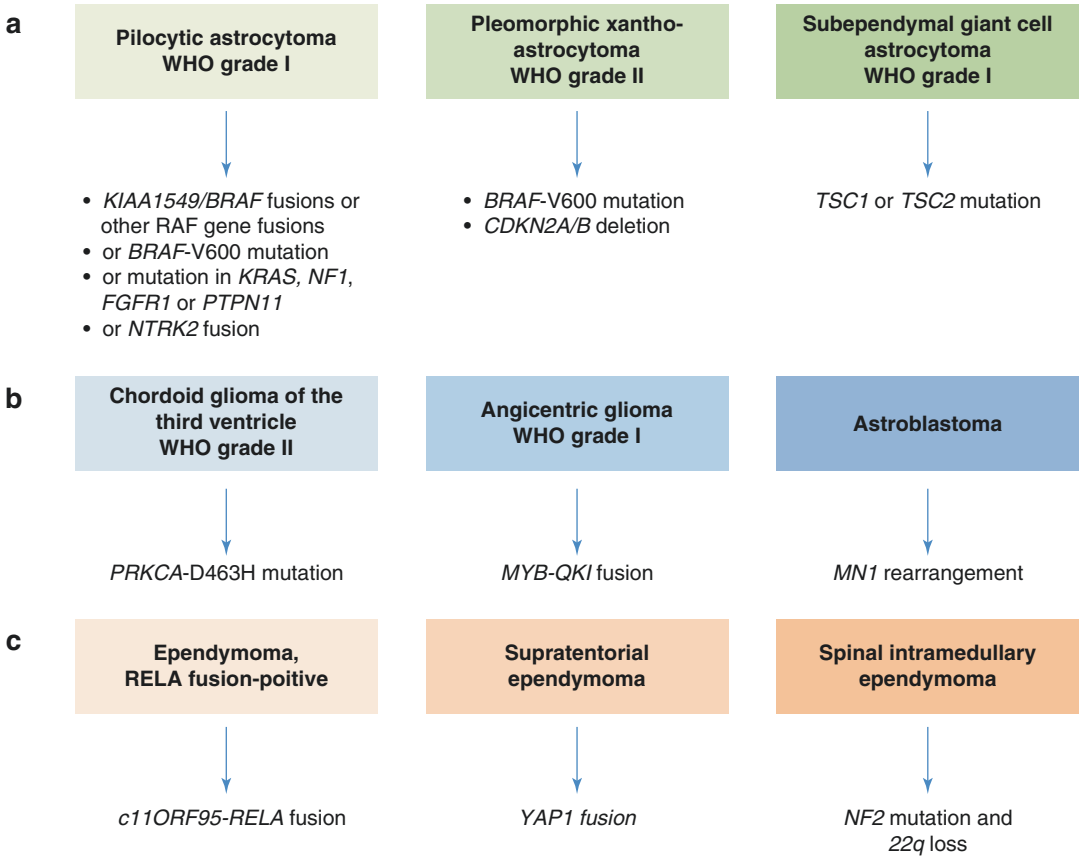

Fig. 1.6 Schematic representation of genetic alterations commonly detected in other astrocytic gliomas (**a**), selected ependymal tumors (**b**), and other gliomas (**c**)

(Fig. 1.5d). In addition, somewhat smaller spindle cells arranged in streams are commonly encountered. Multinucleated cells may be present but true giant cells are rare. Formation of perivascular pseudorosettes mimicking ependymal pseudorosettes is sometimes seen. Calcification is common. Mitotic activity is low. The presence of necrotic areas does not imply malignant behavior. SEGAs correspond to WHO grade I.

Immunohistochemistry. The tumor cells show variable expression of glial (GFAP, S-100) and/or neuronal markers (synaptophysin) (Fig. 1.5e). The MIB1 index is low.

Differential diagnosis. SEGAs primarily need to be distinguished from diffuse astrocytic gliomas, in particular gemistocytic astrocytomas and giant cell glioblastomas. Patients diagnosed with SEGA that are not already known with tuberous sclerosis should be checked for the presence of other manifestations of this syndrome.

Molecular pathology. SEGAs are characterized by biallelic inactivation of either the *TSC1* or the *TSC2* tumor suppressor gene (Fig. 1.6a). This leads to aberrant activation of mTOR signaling, which represents a target for pharmacologic inhibition [49].

1.3.3 Pleomorphic Xanthoastrocytoma

Definition. A well-circumscribed, slowly growing astrocytic glioma with a superficial (meningocerebral) location, histologically characterized by pronounced cellular pleomorphism, xanthomatous tumor cells, perivascular lymphocytes, a

reticulin network around single or grouped cells, and eosinophilic granular bodies. Activating *BRAF* mutation combined with *CDKN2A* deletion is present in most cases.

Incidence and age distribution. Pleomorphic xanthoastrocytomas are rare tumors. Children and young adults are primarily affected. A long-standing history of seizures is common.

Macroscopy and localization. Pleomorphic xanthoastrocytomas are well-circumscribed, often cystic tumors that grow superficially in the cerebral cortex and extend into the adjacent leptomeninges. The temporal lobe is most commonly affected.

Histopathology. Pleomorphic xanthoastrocytomas are relatively compact and well-circumscribed tumors growing in the cerebral cortex and invading the meninges. A fascicular growth pattern is commonly seen. Histologic hallmarks include the presence of pleomorphic, sometimes bizarre, and multinucleated giant cells, lipidized astrocytic tumor cells, eosinophilic protein droplets, often prominent perivascular lymphocytic infiltrates, and a variably dense pericellular/perilobular network of reticulin fibers (Fig. 1.5f–h). The adjacent cortex frequently shows dysplastic features. Rare variants include tumors with angiomatous, epithelioid or gangliocytic/gangliogliomatous components.

Pleomorphic xanthoastrocytoma is a WHO grade II glioma and associated with a relatively favorable prognosis, as indicated by a 10-year survival rate of >70% [158]. However, tumors with five or more mitoses per ten microscopic high-power fields are classified as *anaplastic pleomorphic xanthoastrocytoma WHO grade III* and associate with more aggressive clinical behavior [158].

Immunohistochemistry. GFAP immunoreactivity is generally present but may be variable. S-100 staining is usually strong. Nuclear p53 staining is usually absent or restricted to few cells. A subset of tumors, including rare instances with ganglion cell component, additionally stains for neuronal markers, such as neurofilaments and synaptophysin. Pleomorphic xanthoastrocytomas show frequent expression of CD34 (Fig. 1.5i). Immunoreactivity for BRAF-V600E and loss of nuclear $p16^{INK4a}$ expression are common [74]. MIB1 labeling is low (<5%) in pleomorphic xanthoastrocytomas but increased in anaplastic tumors.

Differential diagnosis. Their superficial location, preferential occurrence in young patients, and typical histologic features distinguish pleomorphic xanthoastrocytomas from high-grade diffuse astrocytic gliomas. The differential diagnosis between anaplastic pleomorphic xanthoastrocytoma and IDH-wild-type glioblastoma, in particular the epithelioid variant, may be difficult, as both share common BRAF-V600E mutations [77]. On the other end of the spectrum, pleomorphic xanthoastrocytoma needs to be distinguished from pilocytic astrocytoma and ganglioglioma, with occasional cases of combined pleomorphic xanthoastrocytoma/ganglioglioma being reported.

Molecular pathology. The characteristic genetic profile consists in BRAF-V600E mutation combined with homozygous *CDKN2A* deletion and loss of $p16^{INK4a}$ expression [74, 134, 158] (Fig. 1.6a). Losses on chromosomes 14 and 22 are more common in anaplastic tumors [158].

1.4 Ependymal Tumors

Definition. Glial tumors with histologic features of ependymal differentiation, including perivascular pseudorosettes and true ependymal rosettes.

Incidence and age distribution. Ependymal tumors account for 1.8% of all primary CNS tumors and for 6.8% of all gliomas [129]. In children, about 5% of primary CNS tumors are ependymal tumors. They may occur at any age but are proportionally more common in children and adolescents.

Macroscopy and localization. Ependymal tumors typically arise along the ventricular system (Fig. 1.2e), including the central canal of the spinal cord. In adults, the frequency of infratentorial versus supratentorial ependymomas is approximately equal, while in children posterior fossa ependymomas are more common. Subependymomas are usually attached to the wall of the fourth or the lateral ventricles.

Myxopapillary ependymomas are located in the conus/cauda region. Ependymal tumors may occasionally grow without relation to the ventricles or even outside of the brain or spinal cord.

Molecular pathology. Recent studies have revealed nine distinct biological subgroups of ependymal tumors, with three subgroups in each anatomical location, i.e., the spinal cord, posterior fossa, and supratentorial compartment [107]. In each location, one prognostically favorable subgroup was designated as molecular subependymoma group that is composed of subependymomas and a subset of classic ependymomas. Among the supratentorial tumors, two subgroups are characterized by fusion genes involving either the NF-κB downstream intermediate transcription factor p65 (*RELA*) or the YES-associated protein 1 (*YAP1*) gene (Fig. 1.6b) [107, 108]. The *RELA* fusion-positive tumors are associated with less favorable prognosis and constitute a separate entity. Among posterior fossa (PF) tumors, the prognostically unfavorable subgroup A (PF-A ependymoma) mainly occurs in children and is characterized by a stable genome. Immunohistochemically, PF-A ependymomas show loss of nuclear H3-K27me3 expression [106]. The second subgroup (PF-B ependymoma) is characterized by chromosomal instability but more favorable clinical behavior [107]. Spinal intramedullary ependymomas carry chromosome 22 deletions associated with *NF2* gene mutations (Fig. 1.6b), while myxopapillary ependymomas often show multiple numerical chromosome aberrations [107]. *RELA* fusion-positive ependymomas and PF-A ependymomas are associated with the worst outcome among all ependymoma subgroups [107].

1.4.1 Ependymoma

Histopathology. Diagnostic hallmarks are pseudorosettes, i.e., perivascular tumor cells extending radial, fibrillary processes toward the vessel wall, and true ependymal rosettes, i.e., canals and tubuli composed of a single layer of cuboidal tumor cells (Fig. 1.7c). Cellular density is moderate and mitoses are rare, while necroses may occur. Ependymomas are usually well delineated from the brain. The *papillary ependymoma* variant shows marked disintegration of areas remote to vessels, leading to a pseudopapillary pattern (Fig. 1.7d). *Clear cell ependymoma* is largely composed of oligodendroglia-like tumor cells with clear, PAS-positive cytoplasm. *Tanycytic ependymoma* features fascicles of spindle cells with elongated processes (Fig. 1.7e). Ependymomas correspond to WHO grade II.

Immunohistochemistry. Tumor cells are positive for GFAP, preferentially around blood vessels. A dot-like perinuclear EMA positivity is typical, while ring-like staining pattern and linear labeling of luminal surfaces are less common. OLIG2 staining is typically negative or sparse in ependymomas. Loss of nuclear immunoreactivity for H3-K27me3 is typical for posterior fossa type A tumors (Fig. 1.7g).

Differential diagnosis. Papillary ependymoma has to be differentiated from other types of papillary tumors, including choroid plexus papilloma, astroblastoma, papillary meningioma, papillary tumor of the pineal region, and metastatic papillary carcinoma. Clear cell ependymoma closely resembles neurocytoma and oligodendroglioma, and diagnosis may require application of immunohistochemistry to exclude neurocytic differentiation and molecular testing for IDH mutation and 1p/19q codeletion to exclude an oligodendroglial tumor. Tanycytic ependymoma may be difficult to distinguish from pilocytic astrocytoma but in contrast to pilocytic astrocytoma lacks OLIG2 expression.

1.4.2 Anaplastic Ependymoma

Histopathology. The most important criterion for anaplasia in ependymal tumors is high mitotic activity, while high cellular density, microvascular proliferation, and pseudopalisading necrosis being also typically encountered. Pseudorosettes are less prominent, and ependymal rosettes are commonly missing in anaplastic ependymomas.

Immunohistochemistry. The immunohistochemical expression pattern corresponds to that of WHO grade II ependymoma.